Appl. Phys. A 80, 575–579 (2005)
DOI: 10.1007/s00339-004-2887-4

Applied Physics A
Materials Science & Processing

D.-Q. YANG
E. SACHER✉
M. MEUNIER

The creation of Au nanoscale surface patterns by the low energy Ar^+ beam irradiation of Au clusters evaporated onto a SiO_2/Si surface

Groupe des Couches Minces and Département de Génie Physique École Polytechnique
C.P. 6079, succursale Centre-Ville Montréal, Québec H3C 3A7, Canada

Received: 16 February 2004/Accepted: 26 March 2004
Published online: 30 June 2004 •

ABSTRACT Ex-situ contact-mode atomic force microscopy (C-AFM) was used to study the evolution of the topography of nanoscale Au clusters, deposited onto SiO_2/Si surfaces, as a function of Ar^+ beam irradiation. Various nanoscale Au surface patterns were created, at an ion beam energy of 2.5 keV, by controlling the ion beam conditions. These patterns include ordered or disordered spheres as well as a nanoporous metal layer. We found that the original ($\sim$ 4 nm) clusters coalesced, under the ion beam, to form both larger clusters ($\sim$ 9 nm) and a nanoporous interphase layer ($\sim$ 6.5 nm). Under continued irradiation, both the original clusters and the nanoporous layer were absorbed into the larger clusters.

PACS 39.29+k; 81.16.-c; 61.46.+w

1 Introduction

Nanostructures are being intensively studied for their size-dependent structural, electronic, physical and chemical properties, which differ from those of bulk materials having the same chemical compositions [1, 2]. Advances in the fabrication of nanoscale devices will depend on improvements in the ability to synthesize, deposit, and position nano-sized building blocks on suitably designed substrates.

Several techniques, employing different strategies, have been used to create patterned nanostructures on surfaces. Some more recent techniques include the electrochemical creation of nanopores [3], block copolymer lithographic templates [4], the localized deposition of material onto [5], or its removal from [6], a scanning probe microscope (SPM) tip, the direct manipulation of deposited nanoclusters using an SPM tip [7, 8], the ion beam irradiation of surfaces [9], the self-assembly of clusters or atoms on surfaces [10], and the deposition of a few monolayers of metals on some substrate surfaces [11]. Previously, we showed [12] that the surface density and size of Cu nanoclusters on HOPG could be controlled by choosing the proper Ar^+ treatment conditions.

In this study, we demonstrate that a few monolayers of Au, deposited onto native oxide Si surfaces, exist as clusters, and exhibit various surface patterns during low energy (2.5 keV) Ar^+ radiation. This is due to the competition among several processes: the enhanced Au cluster coalescence under ion bombardment, the interactions at the Au−Au and Au−SiO_2 interfaces, as well the loss of Au during ion bombardment. These interactions lead to the formation of both a nanoporous layer and larger clusters; ultimately, the nanoporous film is consumed by the clusters.

✉ Fax: +1-514/390-3210, E-mail: edward.sacher@polymtl.ca

2 Experimental

n-type Si(100) was used as the substrate for the Au deposition. The Si surface was first cleaned with ethanol; no attempt was made to remove the native oxide since it would be replaced during the O_2 plasma treatment that would follow. The Si was then treated for 2 min in an O_2 plasma at 5×10^{-2} Torr and 100 W of power, removing the native oxide and creating a new layer of SiO_2 on the surface: FTIR spectra (not shown) indicated the loss of both absorbed water and carbon contaminant from the native oxide. The subsequent deposition of Au was performed in situ, at a base pressure of 1×10^{-7} Torr and a rate of 0.1 nm/s, by using an electron beam evaporator.

Ar^+ irradiation was performed in the preparation chamber of our XPS instrument (VG ESCALab 3, Mk II), using a VG EX-03 ion gun, at a base pressure of 10^{-9} Torr or lower. The working pressure was 3×10^{-6} Torr, the Ar^+ ion beam energy was 2.5 keV and the beam diameter was $\sim$ 5 mm. The angle between the ion beam and the surface normal was 57°, and the ion dose was held in the range of $\sim 10^{13}-10^{15}$ /cm^2 by using the ion gun defocusing control and varying the gas pressure.

Ex situ contact-mode atomic force microscopy (C-AFM) was carried out on a Digital Multimode scanning probe microscope. For these measurements, the integral gain was set at two, the proportional gain was set at three and the deflection set point (the feedback voltage controlling the pressure) was set at zero. Commercially available silicon nitride cantilevers, with a typical spring constant of 0.5 N m^{-1}, a typical tip radius of 10−20 nm and tip half angle of 35°, were used. The scanning rate was 2 Hz, and 512 lines were used per image.

3 Results and discussion

On initial deposition, the Au does not wet the SiO_2 surface, causing it to form clusters (Volmer–Weber growth),

as found by TEM and STM [13]. Our own larger AFM study, from which the present data are taken, shows that the clusters formed on SiO_2 are smaller than those formed on native oxide under the same deposition conditions. Our previous work on chemically modifying the Dow Cyclotene 3022 surface, and its effect on the size of subsequently deposited Cu clusters [14], indicates that this decrease in size signals an increased interfacial adhesion, perhaps due to the presence of surface free radicals on plasma treatment.

Figure 1 shows the C-AFM image evolution of a nominal 3 nm of Au, deposited onto the plasma-treated SiO_2/Si surface. The size distributions of the Au clusters after the ion beam irradiation, found in Fig. 2, were obtained as their AFM-measured heights. This evolution occurred under Ar^+ bombardment as the ion dose was varied. The figures indicate that (1) the as-deposited samples exhibit small, densely packed clusters (Figs. 1a and 2a); (2) they are converted to a porous film (Fig. 1e) before retracting (Fig. 1g); (3) the effective size of the Au clusters, on retracting, shows an increase over the original deposition (Fig. 1g,h); (4) these latter clusters are ellipsoidal, more uniform in size and oriented in the Ar^+ beam direction (Fig. 1g,h); (5) the Au cluster density decreases with continued ion beam irradiation, as material is sputtered.

In order to confirm the surface morphological changes of the Au nanoparticles under Ar^+ beam irradiation, field emission SEM (FESEM) was employed. This necessitated the use of a slightly thicker Au layer ($\sim$ 10 nm), capable of being resolved by the FESEM; the morphological changes were identical to those of the thinner deposit, seen in Fig. 1. Figure 3a shows the FESEM images of as-deposited Au nanoparticles and, Fig. 3b, after nanoporous layer formation. Both the nanoporous layer and larger ($\sim$ 9 nm) nanoparticles are clearly seen.

Figure 4 shows the average cluster size as a function of the irradiation time. It is clear that the average size of the Au clusters first increases with ion beam irradiation, as coalescence and nanoporous film formation occur, before ultimately decreasing, as material loss on sputtering becomes evident. Since sputtering occurs throughout the irradiation, the obvious decrease in size signals that a maximum porous layer size has been attained under the irradiation conditions used.

The morphological changes in Fig. 1 are typical of the ion beam-enhanced cluster surface coalescence process, as we previously demonstrated for Cu clusters on HOPG [12], using the XPS core level intensity ratio technique we developed [15] to evaluate mean cluster size and density. The mean size of the Au clusters, in the present case, depends on the wettability (interfacial interaction) of Au on the surface under the deposition parameters used here.

The enhanced coalescence on short term (a few seconds) irradiation results from the increase in both cluster kinetic and thermal energies on ion impact [12]. The magnitude of this energy increase is very difficult to estimate, due to factors such as the efficiency of energy transfer from the irradiating beam to the cluster, its subsequent fractional transfer to the substrate, beam scattering, the effect of the competing sputtering, and the fact that the partial surface coverage by the clusters changes continuously. However, we can attempt to estimate the energy deposition during Ar^+ irradiation. To do this, we must ignore energy deposition directly to substrate and energy losses due to ion etching. We may then obtain the morphological changes of the Au clusters, during the ion irradiation, as a function of estimated energy deposition, which is shown on the upper abscissa of Fig. 4. We note that the morphological changes can be separated into three region: (1) the coalescence region, below $\sim$ 0.2 eV (about 8 kT, with T at room temperature), in which the energy transferred from the ion to the Au cluster marks the beginning of coalescence; (2) the porous layer region, $\sim$ 0.3 to $\sim$ 3 eV; (3) the reclustering re-

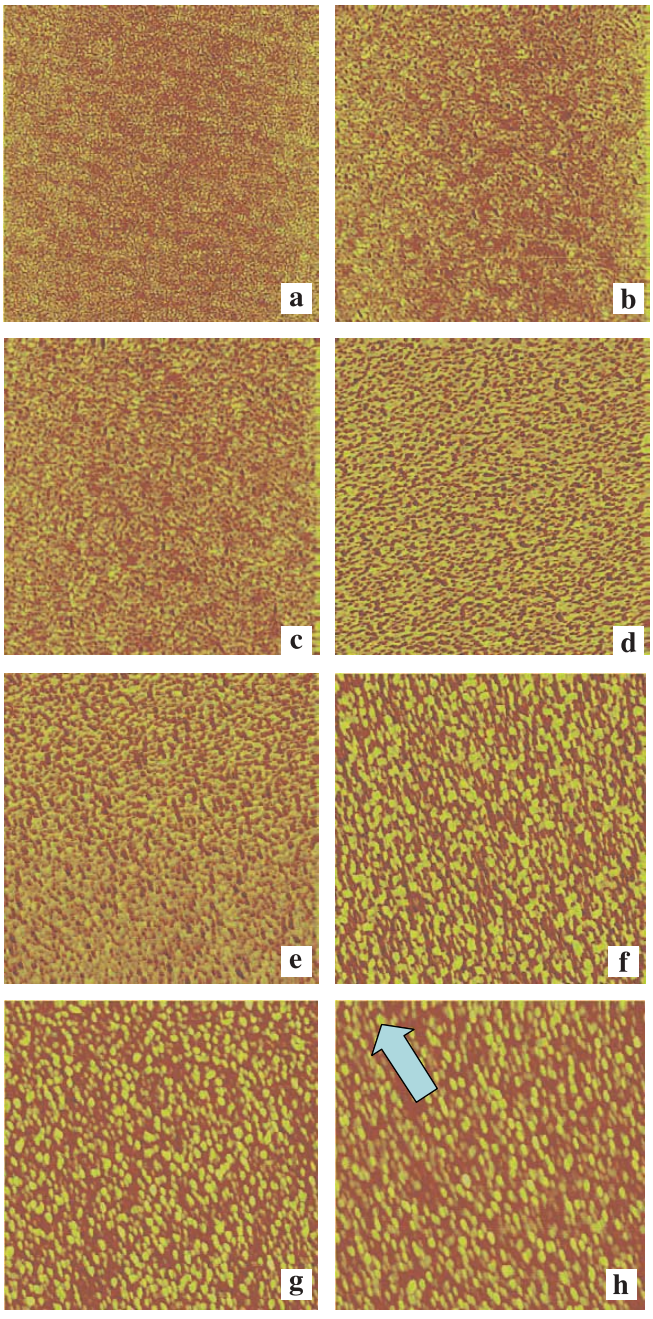

FIGURE 1 Contact-mode AFM images, 2 μm on a side, of clusters formed on the evaporation of a nominal 3 nm of Au onto the SiO_x surface, showing their evolution as a function of beam dose for 2.5 keV Ar^+ for 10 s: **a** as deposited, **b** $\sim 2\times10^{13}$ /cm^2, **c** $\sim 4\times10^{13}$ /cm^2, **d** $\sim 7\times10^{13}$ /cm^2, **e** $\sim 1\times10^{14}$ /cm^2, **f** $\sim 2\times10^{14}$ /cm^2, **g** $\sim 5\times10^{14}$ /cm^2, **h** $\sim 7\times10^{14}$ /cm^2. The *arrow* indicates the ion beam incidence direction

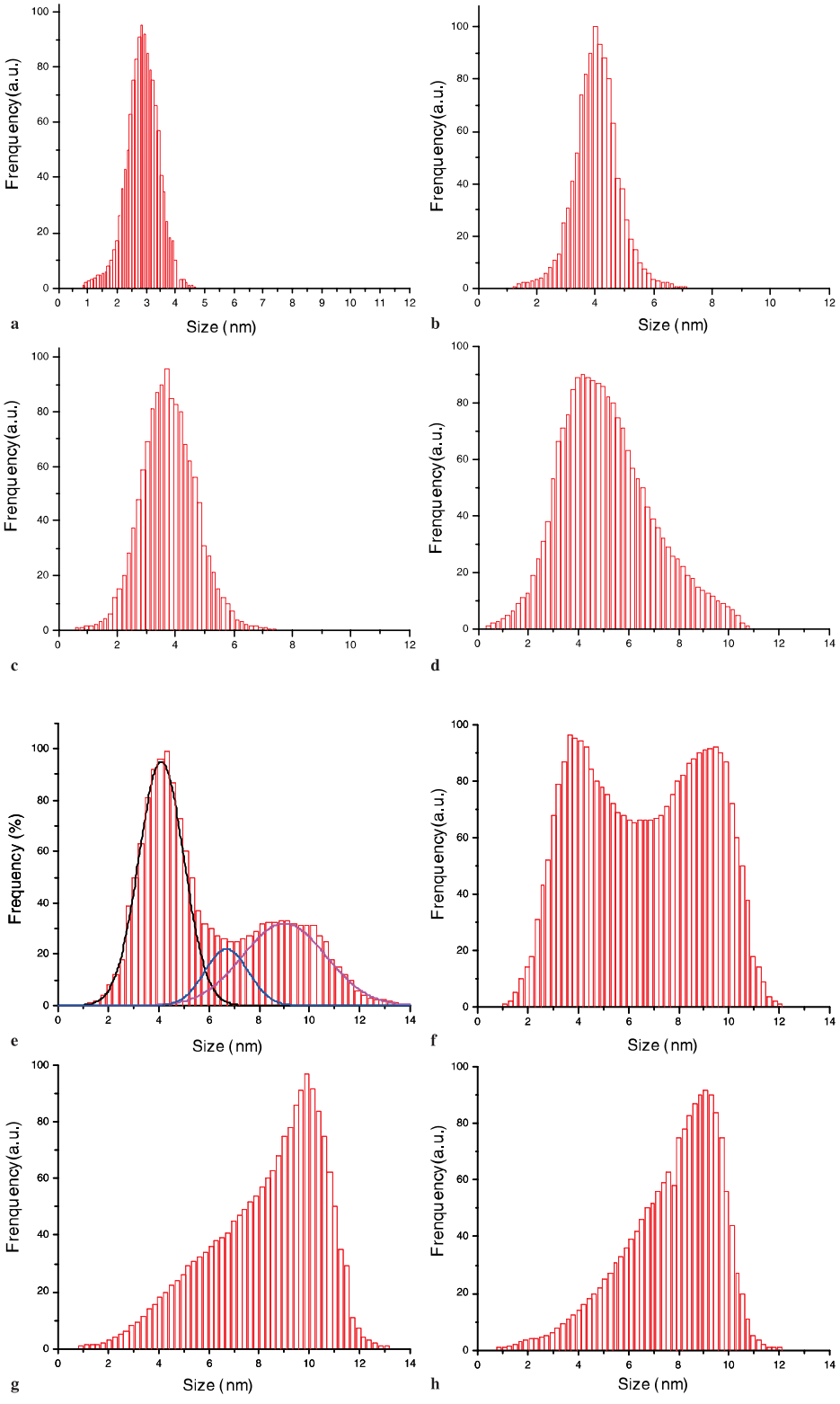

FIGURE 2 Au cluster size distributions, as obtained from AFM-determined heights. Experimental conditions correspond to those in Fig. 1

gion, above ∼ 4 eV, where the porous layer retracts to become larger clusters. Even considering further partial energy loss due to processes not considered, this estimate is still reasonable. This energy transfer causes an increase in kinetic energy, leading to an increase in the cluster coalescence through enhanced surface diffusion, which permits smaller clusters to coalesce more easily [16].

Although both the kinetic and thermal energies transferred by the ion beam impact contribute to cluster coalescence, they may be distinguished, in that only the kinetic energy (delivered at 57°) causes orientation while the thermal energy is random across the surface. We note that the orientation evident in Fig. 1h could only be caused by a transfer of kinetic energy.

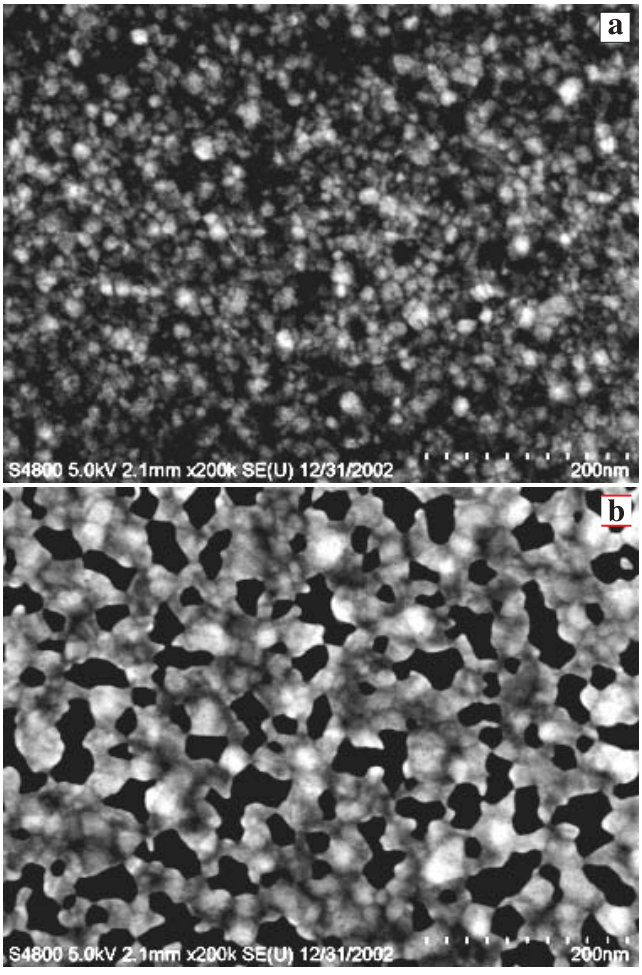

FIGURE 3 FESEM photomicrographs of 10 nm Au on the SiO_x

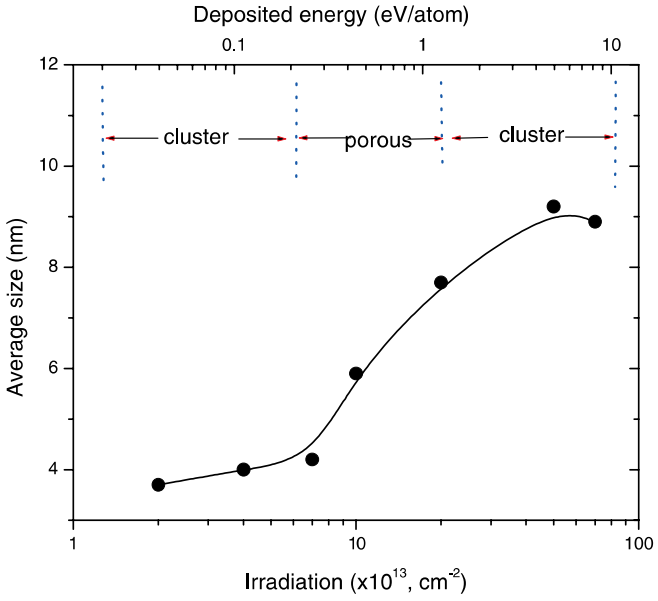

FIGURE 4 Average Au cluster size as a function of Ar^+ beam irradiation dose. The abrupt rise near 7×10^{13} /cm^2 signals cluster contact

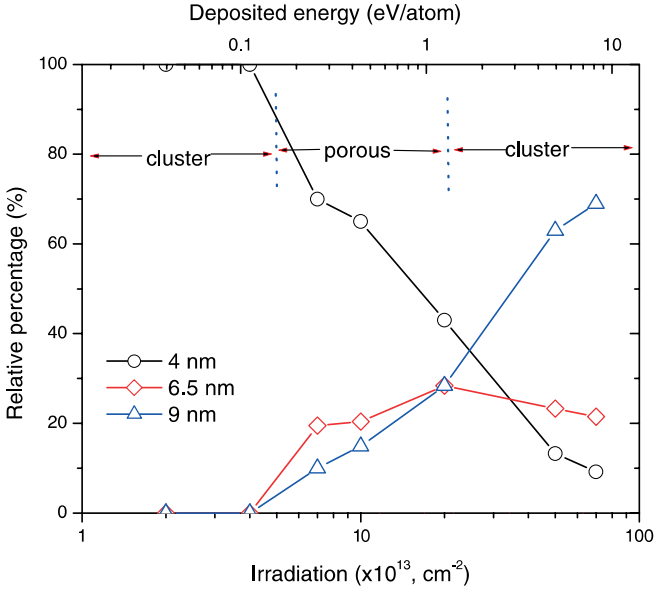

FIGURE 5 Relative percentages of the components of the Au cluster size distributions as a function of Ar^+ beam irradiation dose. Note that the new components appear near 7×10^{13} /cm^2, the onset of cluster contact

It is informative to consider the details of the coalescence behavior as a function of irradiation time: low radiation doses result in a slight increase of the cluster dimension and a narrowing of the cluster size distribution (Fig. 2b); greater irradiation doses cause the appearance of three size distribution peaks, located at ∼ 4, 6.5 and 9 nm in height (an example of the peak deconvolution is seen in Fig. 2e), corresponding to the formation of both larger clusters and a nanoporous interphase layer. The evolution of the average height is found in Fig. 4, while the individual peak evolutions are seen in Fig. 5, with the size distribution progressively shifted to the largest size. This is clear evidence for cluster growth by coalescence rather than through Ostwald ripening.

The behavior of the size evolution in Fig. 5 may be understood as follows: (1) lower irradiation doses result in Au cluster surface diffusion, and some sputtering and coalescence, showing a small size change and a narrowing of the size distribution; (2) the new peaks, appearing at ∼ 6.5 and 9 nm, indicate the onset of coalescence, and the absorption of the ∼ 4 nm clusters into porous film formation (∼ 6.5 nm) and larger clusters (∼ 9 nm); (3) the ultimate growth of the larger clusters, under continued irradiation, absorbs both the remaining original clusters (∼ 4 nm) and the nanoporous film (∼ 6.5 nm).

We may make some crude estimates from these data. Supposing we have hemispherical Au nanoparticles, we find that a 6.5 nm nanoparticle is composed of about four 4 nm nanoparticles, and a 9 nm nanoparticle is composed of about eleven 4 nm particles. The relative number density of the 6.5 nm nanoparticles changes little during ion beam irradiation (Fig. 5) suggesting that what is measured at 6.5 nm is truly a phase, rather than a convolution of 4 and 9 nm nanoparticles.

The ion bombardment may also increase the interfacial interaction between Au clusters and the SiO_2 surface; e.g., the irradiation of evaporated Au atoms was found to promote the reduction of SiO_2 to form Si–Au bonds [17, 18]. We shall explore this in a subsequent paper.

As we previously showed [19], the abrupt increase in cluster dimensions shown in Fig. 4, at an irradiation dose of about 7×10^{13} /cm^2, indicates cluster contact. Thus, both enhanced

cluster coalescence and enhanced cluster–substrate interfacial interaction play important roles in the formation of surface patterns. The enhanced cluster–substrate interfacial interaction observed may be attributed to the increase in defect sites in the substrate (the preferential loss of O introduces Si dangling bonds). Thus, there is a competition between the ion-induced enhanced coalescence of the Au clusters and their reduced surface diffusion due to increased interaction with the substrate surface (as well as material loss on sputtering). As previously shown [12], only cluster coalescence and sputtering occur if there is no change in cluster/substrate surface interaction during ion beam irradiation.

Although some thermal energy, from the ion beam irradiation, may be present to enhance surface diffusion and coalescence, its effect is relatively weak, compared to that of the kinetic energy contribution. For example, coalescence, on annealing Au clusters on SiO_2 has been reported by Arai et al. [20], who found such coalescence to be relatively weak, compared with ion beam-induced coalescence. Further, we previously found that the time-dependent coalescence of Cu clusters, both on annealing and on ion beam irradiation, followed the equation, $d = d_0 t^{\alpha}$, where d_0 is the initial cluster mean size, and α is a constant equal to 0.15 for annealing and 0.33 for ion beam irradiation [14, 21], indicating the increased efficiency of ion beam irradiation over annealing. This has been further confirmed by our recent experimental results on Au clusters on SiO_2 processed by excimer laser irradiation [22], where only thermal energy is transferred: we do not observe nanoporous layer formation, since there is no enhanced Au cluster−substrate interfacial interaction.

4 Conclusions

Our ex situ AFM studies of the surface morphological behavior of Au clusters, on low energy Ar^+ beam bombardment, have demonstrated that various surface patterns can be achieved by ion beam irradiation. Nanoscale surface pattern formation is due to the competition between ion beam-enhanced cluster coalescence and enhanced interfacial interaction. This technique has been shown to be useful for manipulating cluster dimensions, creating nanoscale patterns, making cluster size more uniform, controlling cluster density, and orienting cluster assemblies.

ACKNOWLEDGEMENTS We thank the Natural Sciences and Engineering Research Council of Canada for funding, and Dr. S. Bah for technical assistance with the Au cluster deposition.

REFERENCES

1 H. Gleiter: Adv. Mater **4**, 474 (1992)
2 G.A. Ozin: Adv. Mater **4**, 612 (1992)
3 C.R. Martin: Science **266**, 1961 (1994) ; O. Jessensky, F. Muller, U. Gosele: Appl. Phys. Lett. **72**, 1173 (1998); H. Asoh, K. Nishio, M. Nakao, T. Tamamura, H. Masuda: J. Electrochem. Soc. **148**, B152 (2001)
4 M. Park, C. Harrison, P.M. Chaikin, R.A. Register, D.H. Adamson: Science **276**, 1401 (1997); J.P. Spatz, T. Herzog, S. Mossmer, P. Ziemann, M. Moller: Adv. Mater **11**, 149 (1999); C.T. Black, K.W. Guarini, K.R. Milkove, S.M. Baker, T.P. Russell, M.T. Tuominen: Appl. Phys. Lett. **79**, 409 (2001); M. Park, P.M. Chaikin, R.A. Register, D.H. Adamson: Appl. Phys. Lett. **79**, 257 (2001); B. Koslowski, S. Strobel, T. Herzog, B. Heinz, H.G. Boyen, R. Notz, P. Ziemann, J.P. Spatz, M. Moller: J. Appl. Phys. **87**, 7533 (2000); T. Thurn-Albrecht, J. Schotter, C.A. Kastle, N. Emley, T. Shibauchi, L. Krusin-Elbaum, K. Guarini, C.T. Black, M.T. Tuominen, T.P. Russell: Science **290**, 2126 (2000); J.Y. Cheng, C.A. Ross, E.L. Thomas, H.I. Smith, G.J. Vancso: Appl. Phys. Lett. **81**, 3657 (2002); M. Bal, A. Ursache, M.T. Tuominen, J.T. Goldbach T.P. Russell: Appl. Phys. Lett. **81**, 3479 (2002)
5 C. Baur, A. Bugacov, B.E. Koel, A. Madhukar, N. Montoya, T.R. Ramachandran, A.A.G. Requicha, R. Resch, P. Will: Nanotechnol. **9**, 360 (1998); R. Resch, C. Baur, A. Bugacov, B.E. Koel, A. Madhukar, A.A.G. Requicha, P. Will: Langmuir **14**, 6613 (1998); R. Resch, C. Baur, A. Bugacov, B.E. Koel, P.M. Echternach, A. Madhukar, N. Montoya, A.A.G. Requicha, W. Peter: J. Phys. Chem. **B 103**, 3647 (1999)
6 H. Göbela, P. von Blanckenhagen: J. Vac. Sci. Technol. **B13**, 1247 (1995); H. Göbel, L. Jacobs, P. von Blanckenhagen, J. Vac. Sci. Technol. **B15**, 1359 (1997); U. Kunze, B. Klehn, Adv. Mater. **11**, 1473 (1999); S. Hu, A. Hamidi, S. Altmeyer, K. Köster, B. Spangenberg, H. Kurt: J. Vac. Sci. Technol. **B 16**, 2822 (1998); A. Notargiacomo, V. Foglietti, E. Cianci, G. Capellini, M. Adami, P. Faraci, F. Evangelisti, C. Nicolin: Nanotechnol. **10**, 458 (1999); T.-H. Fang, C.-I. Wang, J.-G. Chang: Nanotechnol. **11**, 181 (2000); U. Kunze: Superlattices Microstructure **31**, 3 (2002)
7 D.M. Schaefer, R. Reifenberger, A. Patil, R.P. Andres: Appl. Phys. Lett. **66**, 1012 (1995); T. Junno, S. Anand, K. Deppert, L. Montelius, L. Samuelson: Appl. Phys. Lett. **66**, 3627 (1995); R. Resch, A. Bugacov, C. Baur, B.E. Koel, A. Madhukar, A.A.G. Requicha, P. Will: Appl. Phys. **A 67**, 265 (1998); M. Andersson, A. Iline, F. Stietz and F. Träger: Appl. Phys. **A 68**, 609 (1999); R. Resch, D. Lewis, S. Meltzer, N. Montoya, B.E. Koel, A. Madhukar, A.A.G. Requicha, P. Will: Ultramicrosc. **82**, 135 (2000)
8 H.W.C. Postma, A. Sellmeijer, C. Dekker: Adv. Mater. **12**, 1299 (2000); M.R. Falvo, J. Steele, R.M. Taylor, R. Superfine: Tribol. Lett. **9**, 73 (2000); S. Hsieh, S. Meltzer, C.R.C. Wang, A.A.G. Requicha, M.E. Thompson, B.E. Koel: J. Phys. Chem. **B 106**, 231 (2002)
9 G. Carter, V. Vishnyakov: Phys. Rev. B **54**, 17 647 (1996); M. Batzill, F. Bardou, K. Snowdon: J. Vac. Sci. Technol. **A 19**, 1829 (2001); R. Gago, L. Vàzquez, R. Cuerno, M. Varela, C. Ballesteros, J.M. Albella: Appl. Phys. Lett. **78**, 3316 (2001); U. Valbusa, C. Boragno, F.B. de Mongeot: J. Phys.: Condens. Matter **14**, 8153 (2002)
10 H. Brune, M. Giovannini, K. Bromann, K. Kern: Nature **451-453**, 6692 (1998); F.M. Leibsle: Surf. Sci. **514**, 33 (2002); R. Plass, N.C. Bartelt, G.L. Kellogg: J. Phys.: Condens. Matter **14**, 4227 (2002); K.-O. Ng, D. Vanderbilt: Phys. Rev. **B 52**, 2177 (1995); A.-L. Barabási: Appl. Phys. Lett. **70**, 2565 (1997); M. Schmidbauer, T. Wiebach, H. Raidt, M. Hanke, R. Köhler, H. Wawra: Phys. Rev. **B 58**, 10 523 (1998)
11 J.T. Moore, P.D. Beale, T.A. Winningham, K. Douglas: Appl. Phys. Lett. **72**, 1840 (1998)
12 D.-Q. Yang, K.N. Piyakis, E. Sacher: Surf. Sci. **536**, 67 (2003)
13 M.J. Rost, D.A. Quist, J.W.M. Frenken: Phys. Rev. Lett. **91**, 26 101 (2003); R.J. Warmack, T.L. Ferrell, R.S. Becker: Physica Scripta **38**, 159 (1988); T. Chinokawa, Y. Ishikawa, M. Kemmochi, N. Ikeda, Y. Hosokawa, J. Kirschner: Surf. Sci. **176**, 397 (1986); J. Wang, C.E.J. Mitchell, R.G. Egdell, J.S. Foord: Surf. Sci. **506**, 66 (2002)
14 D.-Q. Yang, L. Marinu, E. Sacher, A. Sadough-Vanini: Appl. Surf. Sci. **177**, 85 (2001); A. Sadough-Vanini, D.-Q. Yang, L. Martinu, E. Sacher: J. Adhesion **77**, 309 (2001)
15 D.-Q. Yang, M. Meunier, E. Sacher: Appl. Surf. Sci. **173**, 134 (2001)
16 D.-Q. Yang, E. Sacher: Surf. Sci. **516**, 43 (2002)
17 R.S. Bauer, R.Z. Bachrach, L.J. Brillson: Appl. Phys. Lett. **37**, 1006 (1980)
18 S.M. Goodnick, M. Fathipour, D.L. Ellsworth, C.W. Wilmsen: J. Vac. Sci. Technol. **18**, 949 (1981)
19 D.-Q. Yang, E. Sacher: J. Appl. Phys. **90**, 4768 (2001)
20 M. Arai, M. Mitsui, J.-I. Ozaki, Y. Nishiyama: J. Colloid Interface Sci. **168**, 473 (1994)
21 D.-Q. Yang, E. Sacher, in: *Metallization of Polymers 2*, ed. by E. Sacher, (Kluwer Academic Plenum Publishers, New York 2002), p. 97
22 D.-Q. Yang, M. Meunier, E. Sacher: J. Appl. Phys. **95**, 5023 (2004)